TOPOLOGICAL PROCESS DYNAMICS and Applications to Biosystems

{Basic outline material for a seminar(series) on the theme of topological process dynamics in quantum physics and with extensions and applications in biophysics and structural biology)

M. Dudziak

January 30, 1998

Outline of the Seminar

1. Introduction

2. Overview of Topological Dynamics – Quantum, Geometry, and Biosystem

3. P-Adic Numbers and Length Scales

4. The "CHAOITON" Project with JINR and Topologically Stable Solitons

5. A Critical Hypothesis for Biosystems and the Brain

6. Experimental Foundations and Earlier Scanning Probe Microscopy Studies

7. QNET and CLANS – Early Computational Simulations

8. A New Experimental Approach Based Upon Magneto-Optic Sensors and Controllers

9. Recapitulation and Conclusions

(1a)

1. INTRODUCTION

Motivating Questions and Issues

- Is there a problem with our fundamental view of space and time?
- Consider EPR and non-locality and the Quantum Potential (Bohm, Hiley, 1980's)
- There may be only certain allowable (probabilistic) spacetimes and some of them give rise to the dominant (measured) spacetime we call the universe
- Are there only certain allowable or critical geometries and length scales that govern transitions between one spacetime process and another?
- Things may be discretized, and the analytics may be fractal-like or p-adic.
- What kind of connection may exist between quantum events and biological structures and processes, in the brain or elsewhere? (1b, 1c)

Figures 1.1, 1.2 – pages from B&H with AB effect trajectory and QP for AB effect

1.1 (aux)

Page with generalized Schröd. wave eq. and QP eqs. (p. 21 from 9/95 talk)

1(a)

The plan is to describe briefly some theoretical foundations that bring a new orientation to the role of surfaces and multiple 3-spaces at the quantum scale but also at macroscopic scales and in particular for biological systems.

The basis for this approach, called Topological Process Dynamics or Topological Geometrodynamics, is in a view of physical spacetimes (plural) as surfaces in a higher dimensional structure, wherein there is a hierarchy of sheets, as it were, communicating or exchanging energy only at specific points or wormholes (M. Pitkanen, Helsinki). [Note origin of TGD term, fundamentals with MP, references, etc.]

The metric of this complex space H is related to p-adic numbers which come into the picture above Planck length scales. There are implications for hadron string physics and potentially for biology.

The basic p-Adic length scale hypothesis predicts that primes near prime powers of two correspond to physically important length scales:

$L(p) = \text{sqrt}(p)*L0$, p about 2^k, k prime, or a power of a prime.
L0 about 10^4 Planck lengths.

Indeed, $k=13^2=169$ is a power of prime and provides the best fit to neutrino mass squared differences and corresponds also to the length scale associated with the so-called epithelial sheets in the biosystems.

1(b)

Next we will look at the approaches begun first at VCU for two objectives –

First, on the theoretical side, we began to study stability and behavior of 1-D and 1+1 solitons, with colleagues at JINR in Russia, since these were seen as offering some promise for a mechanism by which chaotic and entangled events at the quantum level could give rise to behaviors analogous to elementary particles. The rationale was that, with other evidence of critical soliton-like activity at the macromolecular level (proteins, DNA), this might be a mechanism, and certainly interesting in its own right.

Second, we attempted to define and construct both an experimental platform and computer simulations (against which to compare experimental results and thereby, iteratively, work towards a mathematical model) for investigating how these soliton and biosoliton phenomena could manifest in real biology. The focus was upon neurons and their cytoskeletal and synapto-dendritic geometries, because of a tradition of speculation going back to Eccles, Umezawa, Del Guidice, Stewart, Hameroff, and Penrose. Despite halts in the actual lab work this has led to development of a new approach targeting bioelectromagnetic phenomena and the measurement of changes in cytoskeletal and membrane structures in response to applied electromagnetic influences.

This research has in turn led to some very interesting results in magneto-optics pure and simple, several application designs pertinent to the semiconductor and computing industry, and a new track in biomedical investigation that hopefully will be underway by this summer.

Our goal remains to further develop the theoretical, mathematical foundations, but in the same time to push forward on the applied science and actual real-world applications. The latter have been well compartmentalized into applied R&D and product development.

1(c)

Another Way of Rephrasing the Fundamental Motivating Questions

- Why Is our Universe 3-Space?
  (Or, why do we tend to experience everything in this way and not some other way?)

- Why are there separable objects and processes in the first place?

- Why did living systems develop in the geometry that it has?
  (Why are things in a particular scaling system?)

- What do complex systems work and survive while complicated non-complex ones do not?

- Are computational models of the micro-universe and the cosmos merely interesting analogies or is there something deeper?

2. TOPOLOGICAL DYNAMICS

2.1 QUANTUM PROCESS

We begin with the notion of PROCESS as the source of structure and form

Process algebraic models (Clifford and Grassmann algebras) suggested as a way-out to the problem of non-locality and the integration of QM and Gravity (Relativity)

Process → Flux, Flow, Holomovement [Hiley, 1991]
Flow → Features and Distinctions

Interdependence and potentiality $f_i = f(f_{i-1}) = f(f(f_{i-2}))$ ...

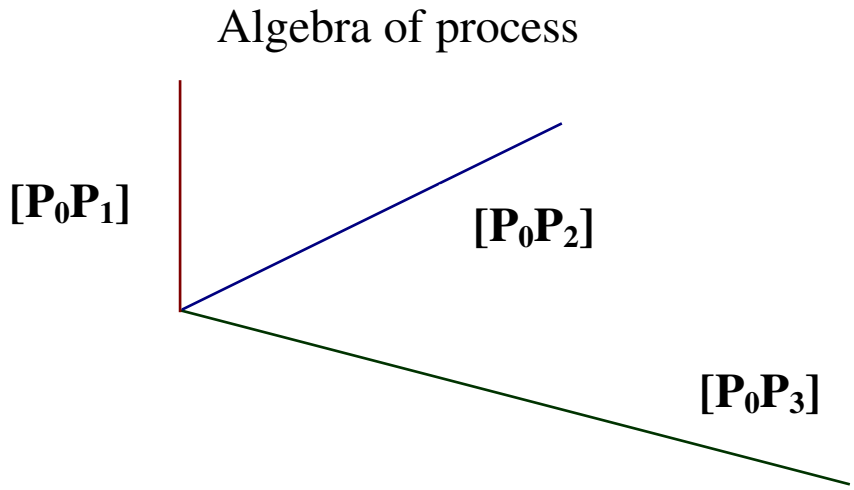

2.2

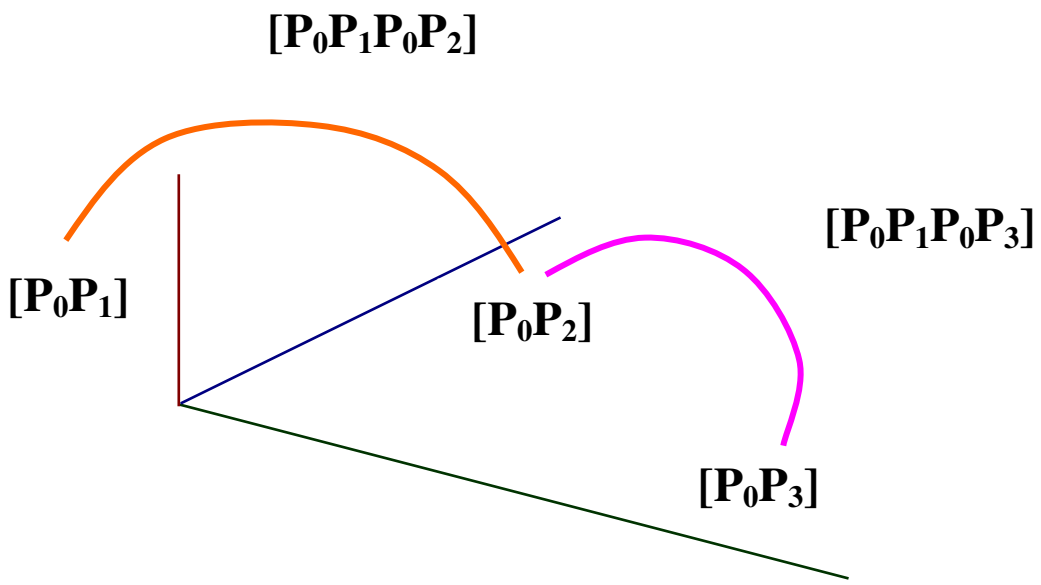

This can be rephrased as [a], [b], [c], [ab], [ac], [bc], such that [ab][bc] = [ac], etc.

Identity processes [aa] = [bb] = [cc] = 1.

[ab][ba] = -[ab][ba] = -[aa] = -1, etc.

[abc][abc] = -[abc][acb] = [abc][cab] = [ab][ab] = -1

2.3

This can be extended to Clifford and Pauli-Clifford algebras which are homomorphic to the SO(3) Lie group of ordinary rotations.

The symplectic Clifford algebra can be generated by bosonic creation/annihilation operators, but this is not about elementary particles but elements of fundamental process.

Picture a Quantum Geometry (Topology) from which a classical spacetime emerges as a kind of statistical average:

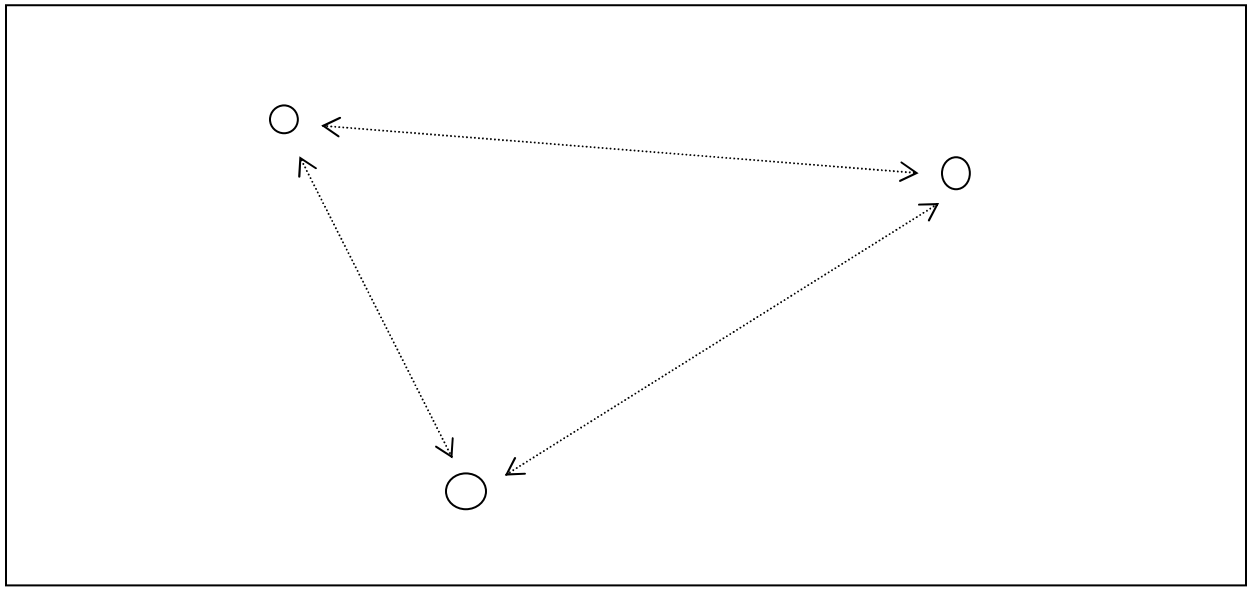

2.4

The POINT persists – it is an idempotent process, p → p

Generation of points is accomplished by $p_1 = Tp_0T^{-1}$ where T = translation operator

Motion (in the PROCESS view) is not a point-to-point sequence in time but an INTEGRATION over a set of points in a phase space [Hiley & Fernandes, 1996] (Similarities to Umezawa's (1993) thermo field dynamics)

Points in classical space are related by some metric imposed from without:

$$p_{i+1} = (x_{i+1}, y_{i+1}, z_{i+1}) = [f_k(x_i), f_l(y_i), (f_m(z_i)]$$

In quantum process, there are different relationships from the dynamics of the space as a whole – a wave function may represent the movement in the vacuum state as a type of thermally induced diffusion, of the form:

$$\Psi(x,t) = \sum\nolimits_E \exp[-\beta E/2]\Psi_E(x)\exp[-iEt/\hbar]$$

2.5 GEOMETRODYNAMICS

Quantum Flux (Pre-SpaceTime) → "Spin Glass" of 3-surface Regions (2a)

Planck-size 3-surfaces glued along boundaries by topological sum
→ sheets and hierarchies of scale

Basic spacetime concept (TGD, Pitkanen, 1985+) is to consider a 4D spacetime surface in an 8D configuration space H = all 3-surfaces of M^4_+ x CP_2 where

M^4_+ = 4D lightcone of Minkowski space and

CP2 = complex projective space of two complex dimensions.

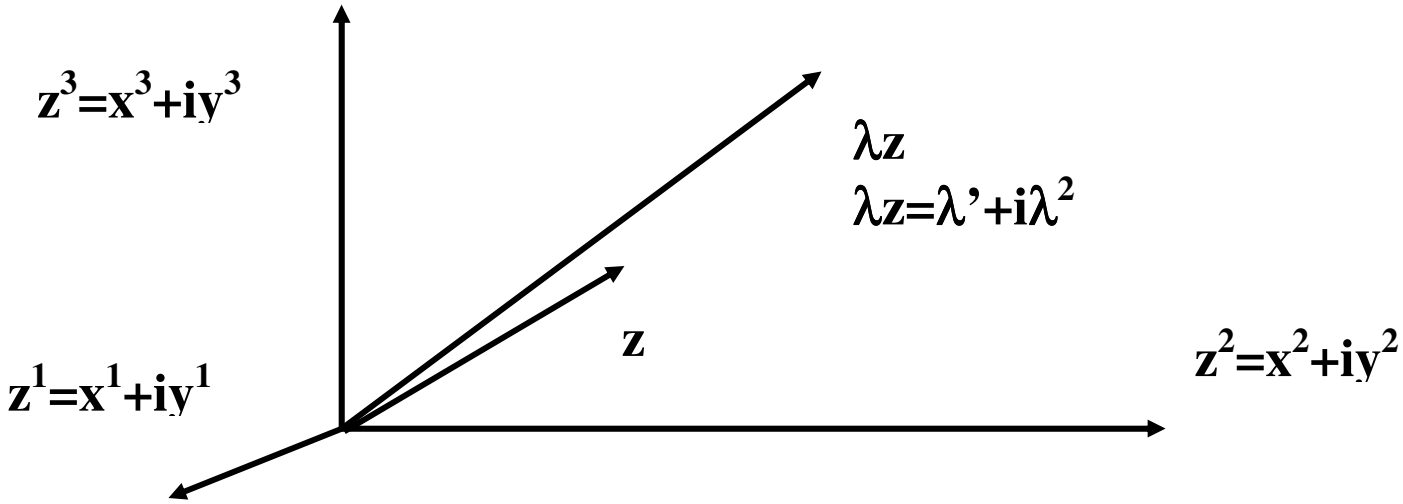

2.6

Two aspects emerge – Poincare invariance of gravitation and a generalization of the string model

Radical generalization of what is a 3-space (3-surface) – there are boundaries and finite 3-spaces within (adjoining) others

Topologically trivial 3-space of GRT → Topological Condensation and Evaporation

2.7
Some Visualizations of Topological-Sum/Difference Particle Dynamics

2.8
Topological Contacts and Condensation Leads to Hierarchies of Spacetime Sheets

2.9

Joins along boundaries → Strong Correlation among Quantum Systems
(A basis for macroscopic quantum systems and quantum coherence in biology)

2.10

Kahler action of electromagnetic gauge flux between spacetime sheets occurs as a charged WORMHOLE with characteristics of S^2 x L.

Implication is that spacetime topology is ULTRAMETRIC below some length scale(analogy to spin glass) such that

$$d(x,y) \leq MAX(d(x),d(y)), \neq (d(x)+d(y)$$

2(a)
We start with a quantum process flux that is pre-space, pre-time, pre-form.
The question is how a stable spacetime with structure emerges from
Something that is No-Thing.

We move to the idea of a spin glass type behavior that is dynamically creating stable vortices or eddies which are defining the elements of what the quantum and classical world is built from. A kind of "virtual world" that is in fact the foundation of the macroscopic "real" world.

These movements can be understood as topological transformations which are the interactions of quantized component spaces with one another resulting in a continuous manifold.

Extremals, fundamental 3-surfaces of Planck scale, can be thought of as fundamental idempotent processes, but by joining and glueing with others at the same scale or higher they give rise to sheets and geometries ultimately behaving at the classical order.

3. P-ADIC NUMBERS AND LENGTH SCALES

3.1

Length Scale Hypothesis

(3a)

$$L(p) \approx 10^4 \sqrt{G}\sqrt{p}$$

Ordinary (real) topology approximates for above L(p), and spacetime sheets of increasing size stay close to L(p).

P-Adicity

Let a real number

$$q = m/n = (r/s)p^{\nu}$$

where r and s are relatively prime to each other and to p, s > 0

$$\varphi_p(q) = p^{-\nu} = \text{p-adic valuation of q}$$

and

$$|x|_p = p^{-\nu} = \text{p-adic absolute value of x}$$

3.2 From p-adic values to metrics (3a)

Every rational x has a "unique" p-adic expansion

$$x = \sum_{j=m}^{\infty} a_j p^j$$

where m=integer, a_j=set of integers between 0 and p-1 inclusive, and sum convergent.

The p-adic metric $d(x,y) = |x-y|_p$ gives rise to the p-adic topology.

Spacetime surface → Regions with different p-adic primes
(each corresponds to a sheet of finite size glued by wormhole contacts)

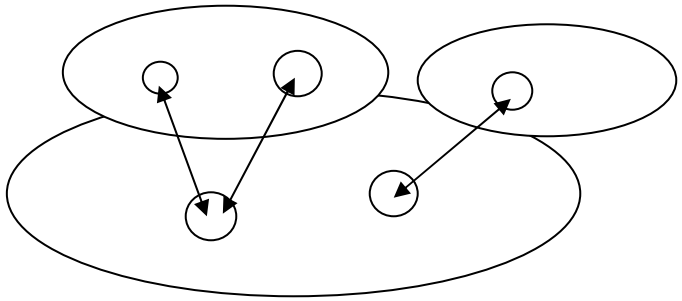

3.3 Why a p-adic topology?

Kähler Action a type of nonlinear Maxwell field
that forms the configuration space geometry and associates unique $X^4(X^3)$ to a given X^3

$$K(X^3) = \text{Min}\ \{S_K(X^4) \mid X^4 \supset X^3\} \qquad (3a)$$

Vacuum degeneracy and nonequivalence →

Something akin to spin glass state degeneracy

DISCONTINUOUS change of physical quantities through 3D surfaces
No Infinite Surface Energies
Like magnetization, but also in time dimension

Discontinuous time? (Suggested in another vein by Finkelstein (Chronons))

3.4 How does the Length Hypothesis Work?

$$L(p) = \text{sqrt}(p) * L0$$

where L0 ≈ CP2 radius, @ 10^4 Planck length.

Elementary particle mass scales as 1/L(p), minimum size L(p)

Below L(p) p-adic physics, above real

FAVORED p-adic primes ≈ 2^m, $m=k^n$, k prime, n integer

Elementary particles (e, μ, τ) ←→ k = 127, 113, 107 (3b)

Elementary Particle Horizon : P-Adic → Minkowskian classical spacetime

3.5

Lipid layers / cell membrane ←→ k=149, 151

Typical cells ←→ k=167

$$L = 2^{(167-151)/2}(10^{-8})m \text{ which is } 2.56*10^{-6}\,m$$

Length scale k=157 ←→ Virus-sized structures

$$L = 2^{(157-151)/2}(10^{-8})m \text{ which is } 3.2*10^{-7}\,m$$

Length scale k=163 ←→ Nanobacteria structures [Kajander, 1997]

$$L = 2^{(163-151)/2}(10^{-8})m \text{ which is } 0.64*10^{-6}\,m$$

Figure 3.1 – 3.4 from MP, TGD-PAD book (figures 2.2 – 2.5, chapter 2, pp. 44-47)

3(a)
There are several factors involving p-adic numbers and metrics.
First there is the Quantum p-adicity below a minimum scale where p-adic topology applies.

Space of minima of free energy is ultrametric, obeying N(x+y)<= Max(N(x), N(y))
& p-adic number are completion of rationals, one for each prime.

Second there is the p-adic length scale hypothesis and the relationships that seem to hold between sizes of different spacetime sheets (particles, viruses, bacteria, cells, … astronomical objects…)

(3.3) Consider all possible X4 with X3 as submanifold, X3 $\subset$ X4. If X3 has a boundary then it belongs to boundary of X4. Associate to each X4 the Kahler action which is analogous to a minimum of thermodynamic free energy, changing discontinuously when some config. space coordinate changes, a kind of phase transition or catastrophe action.

3(b)
From M. Pitkanen, padic2.html:

Elementary particle masses are proportional to 1/sqrt(p) and hence exponentially sensitive to the value of k. It is however possible to associate unique primes k to the known elementary particles. For instance, electron, muon and tau correspond to the subsequent (!) primes k=127,113,107.

Predictions are correct with few per cent and renormalization effects give an explanation for the small discrepancies. TGD provides an explanation for CKM mixing as basically due to the mixing of the boundary topologies of quark like 3-surfaces.

The requirement that CKM matrix satisfies empirical constraints fixes U and D matrices and quark masses and leads to correct predictions for hadron masses. The scenario solves also the spin crisis of proton and so called R_b and R_c anomalies of electroweak standard model.

4. “CHAOITON” – Chaotic Solitons in 1+ Dimensions

4.1

Independently we were noticing the phenomenon of solitons and their application to elementary physics and to biological energy transport.

Could a soliton structure be at work providing STABILITY in topological processes at different scales?

Could a soliton formalism in 3D model the type of wormhole gauge flux that would sustain the topological identities and structures of spacetime 3-surface sheets in condensation and evaporation processes?

Would such solitons be similar across particle physics, protein/DNA conformation, and microtubule-constrained energy transport in cells?

First we had to examine whether certain apparent solitons were really non-trivial and non-degenerate.

4.2

Objective

Numerical and analytical investigation of particle-like soliton solutions :

- Lorentz-invariant classical field theories
- Broken internal symmetry,
- Allowing for {D=1,2,3} topological solitons

Conjecture

3D particle-like solitons "built" of unit isovector, spinor, vector fields in some type of classical approximation

Key Focus

Sigma-models – unit isovector n(x) field

Particle and nuclear physics	Superfluid He phases
High-temp superconductivity	Ferroelectrics and magnets
Macromolecule chains (DNA, protein)	

4.3

2D Sigma Model in Isotropic Heisenberg Antiferromagnet

Langragian

$$L = \frac{1}{2}\partial_\mu s_a \partial^\mu s_a = \frac{1}{2}\left[(\partial_0 s_a)^2 - (\partial_k s_a)^2\right]$$

with: $s_a s_a = 1$ $\mu = 0, 1, 2$ $k = 1, 2$ $a = 1, 2, 3$

Hamiltonian

$$H = \frac{1}{2}\left[(\partial_0 s_a)^2 + (\partial_k s_a)^2\right]$$

Time-dependent

$$\partial_\mu \partial^\mu s_i + \left(\partial_\mu s_a \partial^\mu s_a\right) s_i = 0, \quad i = 1,2,3,$$

Stationary

$$\partial_k^2 s_i + \left(\partial_k s_a\right)^2 s_i = 0$$

4.4

Using the (θ, ϕ) form of dynamic equations, we investigated Belavin-Polyakov (BP) solitons:

$$\theta_s(r,R) = 2\arctan\left(\frac{r}{R}\right)^m, \quad \phi_s = m\chi$$

$$r^2 = x^2 + y^2, \quad \cos\chi = \frac{x}{r}, \quad \sin\chi = \frac{y}{r}$$

Stationary topological BP solitons are stable independent of topological index Q_t

Next question →pair interactions under collisions.

Solitons in 2D anisotropic AFM differ from stationary BP solitons in isotropic AFM/FM only by rotation in internal space at frequency **ω**.

We investigated x = 0, $\omega^2 < 1$, and $\omega^2 = 1$, and found dynamical topological solitons only at $\omega^2 = 1$.

Figures 4.1 – 4.9

Slides and transparencies of Sine-Gorden et al (MATLAB, etc.)

Fundamental Solitons
Sketches from book
Standard atan (2), Bell-type (2), Singularities (1)
Conjecture
What about weak instability?

5. A Critical Hypothesis for Biology

5.1

Quantum Topological Events

Wormhole-like CP2 extremals operating between contiguous spacetime sheets

- occurring as type of CA or spin-glass phernomenon
- analogous to massively parallel computations
- superconductive pathways within phospholipid lattices

Generate 2D / 3D soliton behaviors that propagate through actin to MT networks

Create quasi-crystalline formations with intracellular and intercellular ranges

Acting as “quantum antennae” sensitive to minute changes and disturbances

Enabling quantum-scale coherence and superconductive signal propagation

5.2

A Radical Hypothesis

Disturbing the Classical Reductionist (Non-Complex) Model

Disturbs the Standard Cell Biological Model including the Position of DNA and the Nucleus

Opens the Door to Plausibility of Boundary Conditions and Cell / Organ GEOMETRY having a significant role in the picture of metabolism, pathology, morphogenesis, and more complex processes (learning, auto-immune recognition, intelligence…)

Opens the Door to Some Really Bizarre (from the Classical Perspective) Possibilities of Influence and Communication in the Organic World…

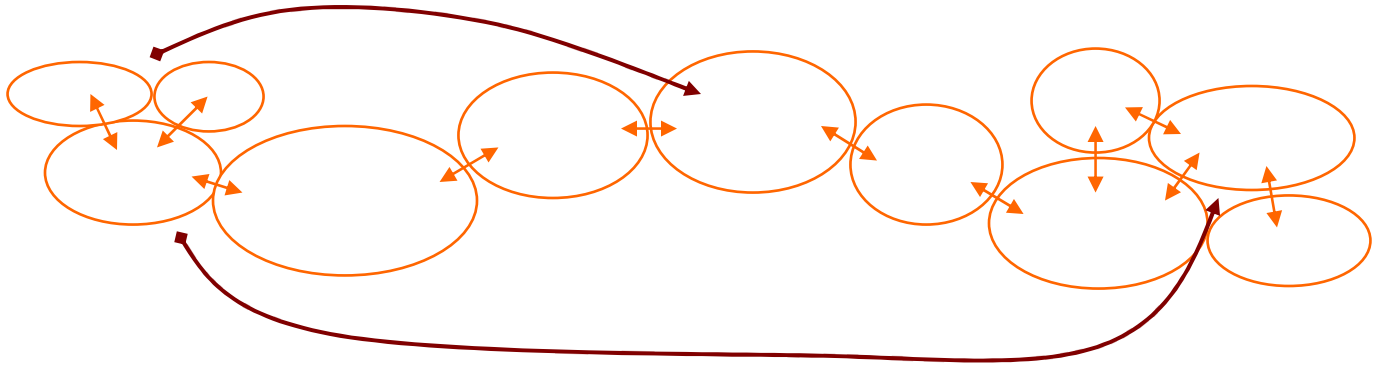

5.3
Convergent Streams of Evidence and Theory

- Microtubules as Computational (CA) Networks
(Rasmussen)

- MT as Information Processing Networks
(Koruga, Hameroff, Penrose)

- MT as Cytoskeletal Regulators of Form and Function
(Established cell biology)

- MT as Quantum Lasers
(Del Guidice, Vitiello, Yasue)

- MT as Quantum Antennae
(Pitkänen)

Nonvanishing Vacuum Gauge Current (EM or Z0 or Both) → BE Condensates
Wormholes serve as conduits between spacetime sheet of surrounding water (Debye layer) and spacetime sheet of the MT, protein, DNA.

5.4
Additional transparencies from earlier talks

MT structure

Dimer polarities

MT cellular automata models

5(a)

6. Experimental Foundations – Neurons and Nanoscopes

6.1

Objective

Study real-time changes in:

- neuron topology
- dendritic growth and interaction
- boundary behavior
- cytoskeletal (MT) geometry

based upon modulation of electromagnetic fields
applied within the cell culture environment

Approach

Cell cultures (neuronal, glial) observed through Atomic Force Microscopy
Construction of controlled growth and EMF measurement apparatus

Environment

Nanoscope III SPM with AFM, Bioscope

6.2

Atomic Force Microscopy (AFM)

Nanoscope-III Multimode AFM with AS-12 “E” Scanner

Range: X-Y 10µm by 10µm Z 2.5µm

(1) Contact Mode
Silicon Nitride Cantilever
- Force (or Spring) Constants 0.58, 0.32, 0.12, 0.06 N/m*
- Nominal Tip Radius of Curvature 20 - 60nm
- Cantilever Lengths 100 & 200µm
- Cantilever Configuration V-shaped

(2) Tapping Mode
Silicon Cantilever
- Force (or Spring) Constant 20 - 100 N/m
- Resonant Frequency 200 - 400kHz
- Nominal Tip Radius of Curvature 5 - 10nm
- Cantilever length 125µm

Figs. 6.1 – 6.3 Hand-drawn AFM transparencies
or
Slides (set 1; from Park Scientific)

6.3

Neural Imaging

XR1 Xenopus Retinal Glial Cells

Preparation: (6c)
ECL (entactin, collagen, and laminin) treated glass cover slips
Constant 60% L15 buffer.

Imaging on:
- Nanoscope III with 10μm^2 Scanner and with Fluid Cell
- Bioscope with Axiovert 135 Zeiss inverted optical microscope
  (@ Lab of E. Henderson, Iowa State, assistants M. Galardi, C. Mosher)

Planned objectives:
- Obtain large set of AFM cell images
- Obtain confocal images of MT network (re: Henderson AFM-Confocal Microscope)
- Extract MT feature maps
- Characterize MT network geometries
- Modulate cell cultures with variable EMF applied in-vitro

Figs. 6.4 – 6.9
Transparency images of Neurons from Bioscope work (MG, Iowa)

6.4

A much better quality set of images

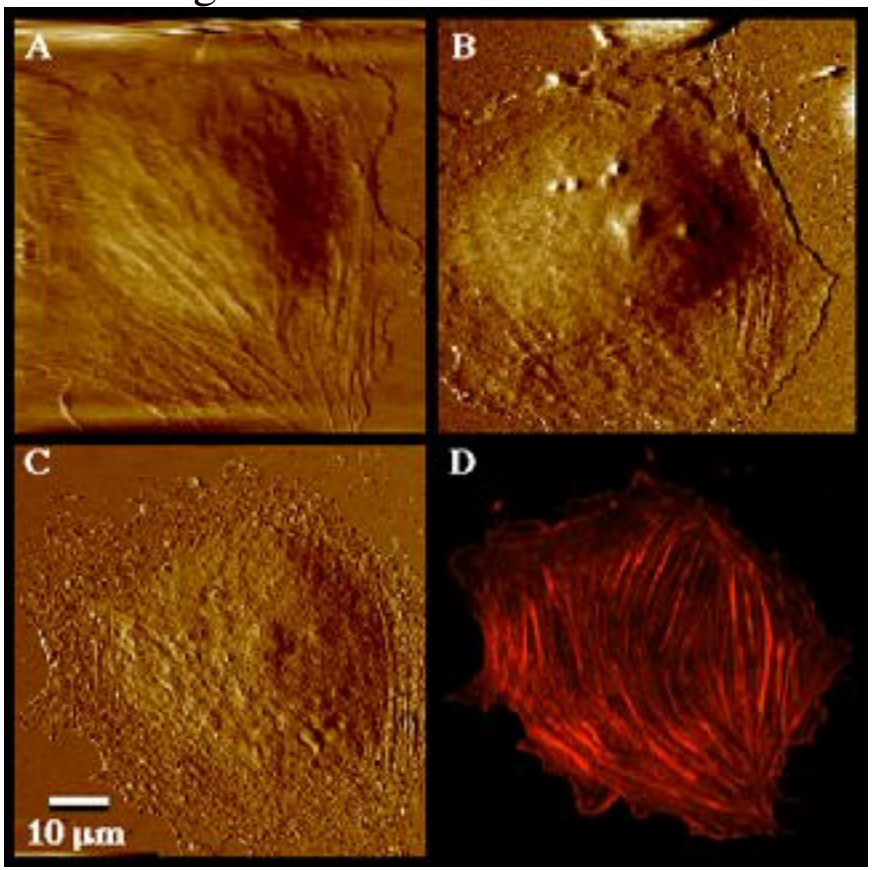

[from http://www.bioforcelab.com/biotech/figs.html]

Live and fixed Xenopus laevis retinal glial XR1 cell imaged by AFM. High pass filtered contact height mode (A) and TappingMode (B) images (living cell). (C) is deflection mode image of cell after fixation. (D) shows the same cell imaged by scanning laser confocal microscopy after staining of f-actin with rhodamine-phalloidin. There is a strong correlation between fiber-like features in the AFM image and actin filaments in the confocal image. Scale bar = 10um. (6c)

6(a)

Notes about cell cultures:

Original plans:

Established clonal cell line, PC-12, originally derived from a rat adrenal pheochromocytoma []. PC-12 cells exhibit many characteristics of neural cells and have been used extensively as a model system for neurobiological and neurochemical studies. These cells transport, store, and release the neurotransmitters norepinephrine and dopamine [] and express sodium action potentials []. They are responsive to nerve growth factor (NGF), a 130 kD protein which arrests the mitotic process and causes the cells to extend long neuronal processes (the differentiated phenotype) []. Removal of NGF causes the cells to revert to the proliferative phenotype.

Stock cultures maintained in T-25 flasks in D-MEM/F-12 medium supplemented with 10% horse serum, 5% fetal bovine serum, and antibiotics in a water-saturated, 5% CO2 atmosphere. For AFM experiments the cells will be trypsinized and seeded at known densities onto circular (12 mm diameter) microporous polycarbonate membranes in special culture dishes (Costar Snapwell Transwell inserts). The membranes are treated to promote cell attachment and growth. If differentiated cells are required, the D-MEM/F-12 medium will be supplemented with 2.5S NGF (the active subunit) at a concentration of 50 ng/ml.

For AFM experiments using live cells, the membranes will be removed from the inserts, backed with a 12 mm round glass coverslip, and mounted in a perfusion chamber for imaging as described below. The cells can also be fixed on the membranes using standard procedures for electron microscopy and imaged as dry preparations. Presently this is accomplished using fixation in 2.5% glutaraldehyde in 0.1 M sodium cacodylate buffer at pH 7.2, progressive dehydration in ethyl alcohol, and air drying from hexamethyldisilazane. The fixed membranes will be detached from the inserts and taped to the magnetic puck for AFM imaging of membrane features and cytoskeletal structures.

6(b)

For comparative purposes some experiments will utilize a patented human neuronal cell line, hNT, available from Stratagene Cloning Systems, Inc. These cells express different neuronal markers and receptors than PC-12 cells (4,5). They will be cultured as stock NT2 precursor cells and differentiated to the hNT neuronal phenotype with NGF as described for PC-12 cells. It is felt that the use of established immortal cell lines in lieu of primary neuronal cultures offers several advantages for these studies. First, a ready supply of pure cell types can be maintained at relatively low cost. Second, the differentiated phenotypes share several significant large-scale structural and physiological characteristics with primary neurons; these basic similarities can reasonably be expected to extend to the nanoscale level. In addition, the ability to control neurite outgrowth (axon-like extensions) by treatment of the proliferative cells with NGF offers the possibility of producing synaptic connections with a variety of target cells or with one another (3). This may be a useful feature for experiments in which the properties of large synaptodendritic fields are to be investigated. Part of this study will investigate methods for controlling the formation of these multicellular structures using the differentiable cell lines and NGF.

AFM Studies of Live Cells (Perfusion Chamber Studies)

In order to study dynamic changes in the structural features of cultured neuronal cells as a function of their chemical environment, live cells grown on polycarbonate membranes as described above will be mounted in the glass perfusion chamber provided by Digital Instruments for use with the Nanoscope. The coverslip-backed membrane forms the floor of a closed flow-through cell which provides for the mounting of the AFM scanning tip within the chamber itself thereby allowing the cells to be imaged in physiological solutions. This chamber will form part of an open-ended system (similar to an HPLC flow line) through which HEPES-buffered culture medium maintained at 37 oC and pH 7.4 will be pumped. This system will allow the cells to be exposed to programmed alterations in medium constituents, e.g., ionic concentrations, and simultaneously scanned to record changes in cell structure.

6(c)

XR1 glial (Xenopus retinal ganglion) cells were grown in culture according to the protocol of Sakaguchi, et al. (56, 55). Briefly, cells are harvested from tissue culture flasks and resuspended in culture media, then plated onto a modified 60 mm culture dish which housed a 30 mm round glass cover slip (in some cases cells were grown on free coverslips). The glass cover slip was pre-treated with ECL (entactin, collagen, and laminin) which promotes flattening and adherence of the cells to the surface. Cultures were incubated at room temperature in ambient atmosphere. Prior to imaging the cells, the culture media was gently aspirated from the preparation and replaced with sufficient protein-free 60% L15 media to cover the cells. For experiments with fixed cells a solution of 4% paraformaldehyde in 0.1M phosphate buffer (pH 7.3) was added, the sample was washed three times, and the cells were stained with rhodamine-phalloidin for 30 to 60 minutes in the dark 25, 55).

For live cell work the petri dish was transferred to a rigid sample holder having a small aperture for optical viewing. A triangular 200 µm long, 20 µm wide cantilever with pyramidal tip was mounted in the BioScope fluid cell holder, positioned in close proximity to the sample (~50 µm) and engaged automatically. All AFM images were taken in 60% L15 buffer. After fixing and labeling with rhodamine-phalloidin the sample was rinsed with phosphate buffered saline (PBS) and imaged with the confocal microscope. Bright field images were acquired using a fiber optic light source reflected from a 45° one-way mirror mounted on the scanning piezo. Non-confocal epifluorescence images were generated by conventional optics. Optical data were captured with an integrating CCD camera and stored in digital format on a Macintosh IIci computer using NIH Image software (version 1.55) and a frame grabber board (Data Translation, Inc., Marlboro, MA).

7. QNET : Quantum Networks and the CLANS : Cellular Local Area Nets

7.1 Objective

Computer simulation of network-like growth at multiple (2+) scales

Modeling quantum-like field behavior and soliton-like wave propagation through constrained geometries (synapto-dendritic spaces)

Modeling boundary/topology-driven discontinuities and coherence as predicted (or conjectured) by TGD and generic TD

Creation of a tool by which to search for interesting behaviors observed in AFM and Confocal Experiments, and by which to refine a mathematical model of the cellular dynamics of real biology

7.2
Approach

PC-based programs, C/C++, MATLAB

Starting from platform of fractal, CA, and neural-network-like algorithms

Incorporation of CSP parallel processor paradigm:

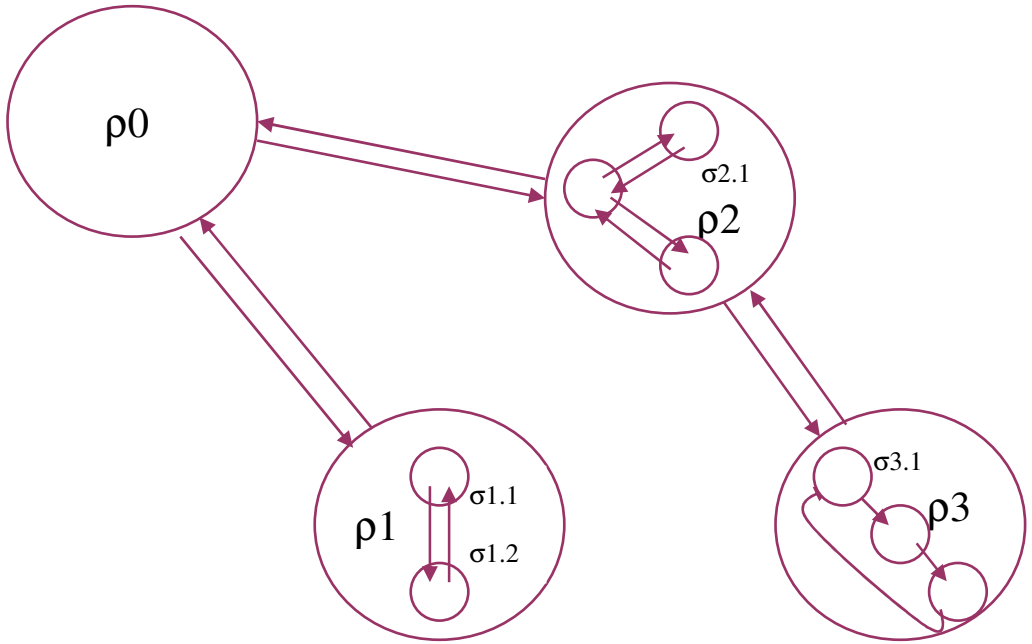

Figs. 7.1 – 7.3
Sketches (hand-drawn transparencies) and GEO / CELL programs

Figs. 7.4 – 7.6
From thesis – Figs. 2.5 (QCAM Configuration), 2.6 (QCAM Clan in Action), and 2.10 (X-operator and multiple regions of pfocess network)

8. New Experimental Approaches and Tools

8.1

Controlled Growth of Cell Cultures

Synthetic Neural Networks

Micro-Machined Electromagnetic Arrays

AFM, Optical and Confocal Microscopy Real-Time

MFM and Magneto-Optic Scanning

Continuous Observation in Three Modes (AFM, Optical, Magnetic)
Of Defined Cellular Topologies Exposed to Differentiable EMF Patterns

8.2
Controlled-Growth Geometries of Cell Cultures

Goals

Long-term cultures
Self-assembled monolayers
Defined Pathways
Neuronal axon and dendrite polarities
Functional synapses
Regulated populations for analysis of transmitter and ion uptake levels

Methods

Chemical and UV Lithography Preparation

EDA (N-2-Aminomethyl-3-aminopropyl trimethoxysilane)
DETA (Trimethoxysilyl propyldiethyylenetriamine)
PEDA, TMA, CL, BIPY
Surface preps with PL (Poly(L-Lysine) and HS (Heparin sulfate glycosaminoglycan)

Significant pioneering advances by J. Hickman & D. Stenger (NRL)

8.3
Micro-machined or SLM-Controlled Arrays for Controlled-Geometry EMF

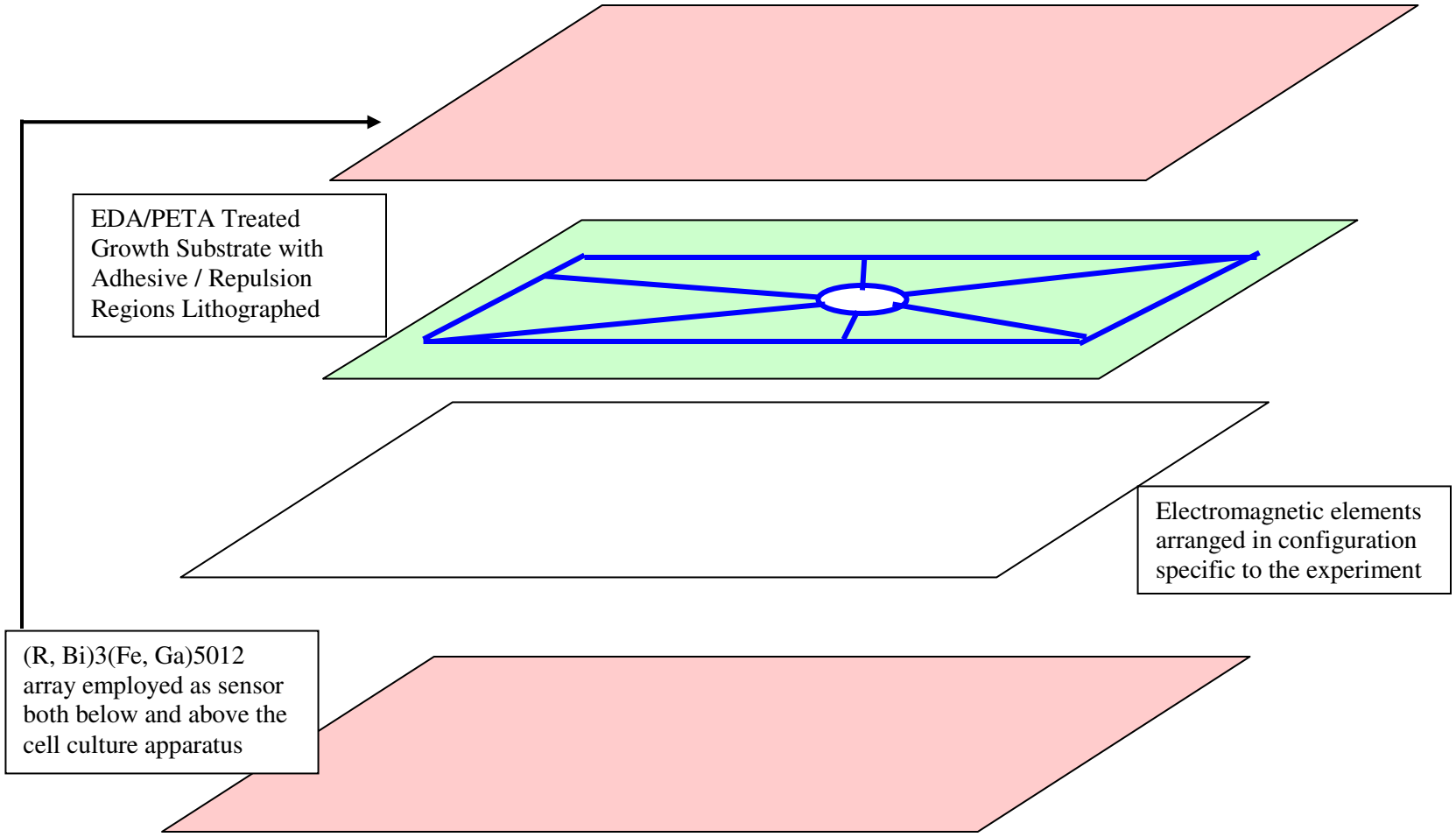

8.4
Imaging with AFM and Confocal Instrumentation

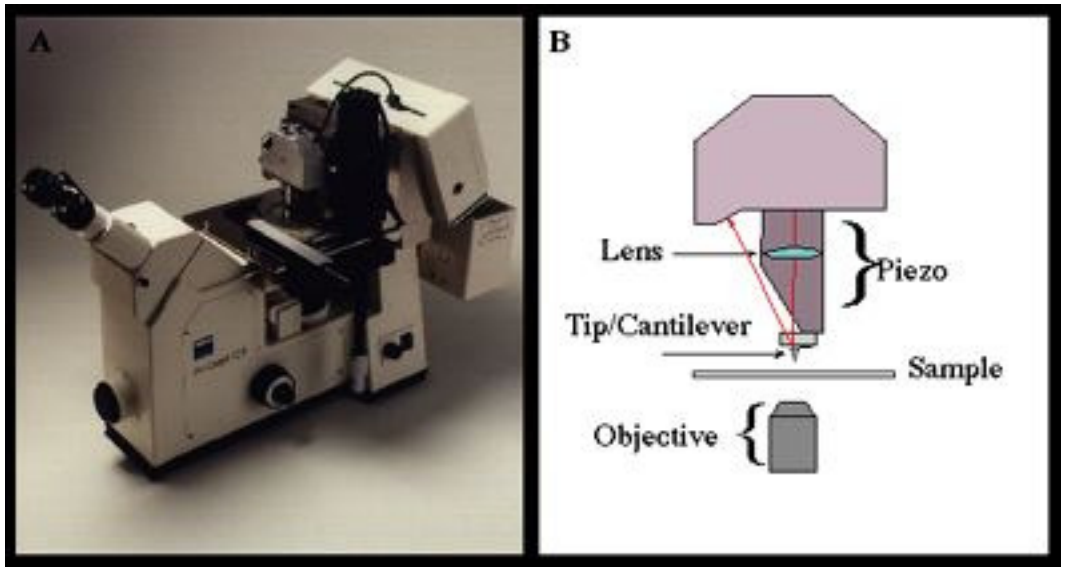

[from http://www.bioforcelab.com/biotech/figs.html] An integrated optical-atomic force microscope. (A) Combined inverted optical microscope (Axiovert 135, Zeiss) and MultiMode AFM (BioScope, Digital Instruments). (B) Optical and AFM images can be obtained simultaneously. This is possible because of the coaxial arrangement of the AFM scanner and the objective lens of the optical microscope.

8.5

MFM and Magneto-Optic Scanning

MFM an established technology, but limited by AFM architecture

MFM prevents simultaneous Tapping-Mode AFM

Fe-Ga Magneto-optic thin-films could open a new dimension for measuring fields in such experiments as are proposed:

- EMF source apparatus
- Cell culture ambient environment

8.6
General composition of MODE thin-film wafers

$$(R, Bi)3(Fe, Ga)5012$$

R = Y, Lu, Pr, Gd, Tm, Yb, Er, Ho, Dy, Tb, Eu

Process

grown by epitaxial layering
Bi_2O_3-PbO-B_2O_3 solvent and garnet-forming oxides,
@ 940-1108 K temperature.

General MO characteristics

Saturation magnetization $\mu Mo = 0 \ldots 1000G$
Specific Faraday Rotation $\Theta F = 2.3$ grad/μm
Absorption Coefficient $\alpha = 0.35 \ldots 0.40$ dB//μm
Max. domain wall velocity V = 200 … 2800 m/s
Coercivity < 0.1 Oe
MO Figure of Merit $\Psi = 2\Theta F/\alpha > 10$ grad/dB
Lattice parameter ≈ 1.25 nm

8.7

Some Images Produced with MagVision Scanner Prototype
(PAL Video → Winnov VIDEUM PC Video Board (ISA bus)

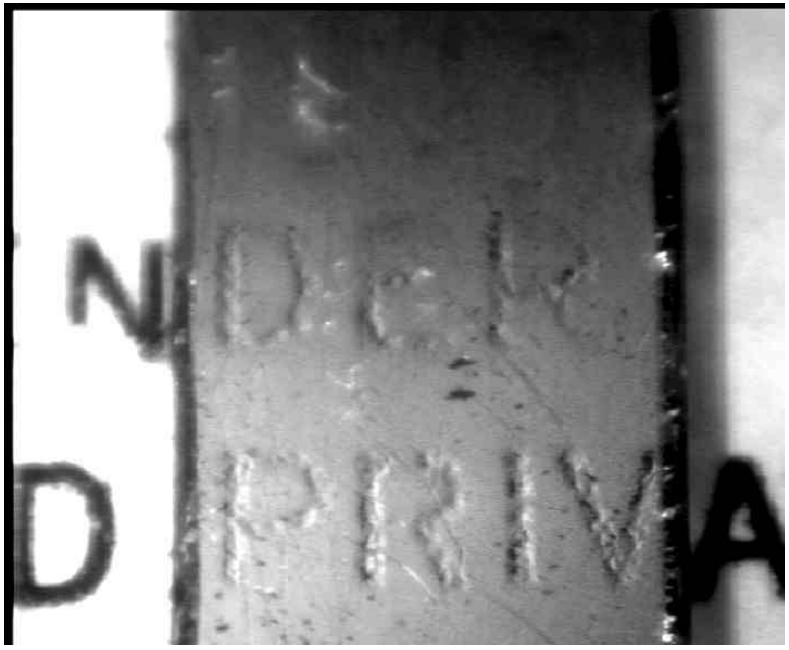

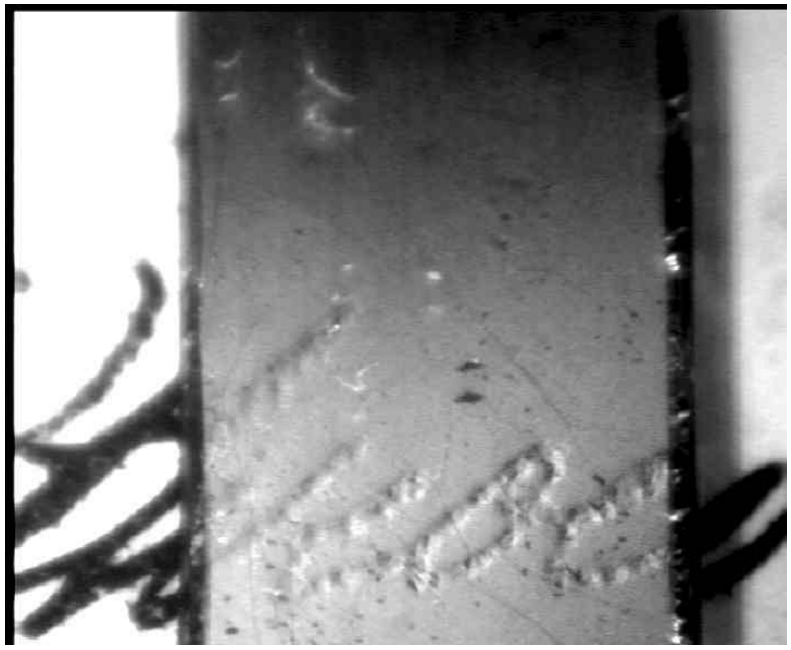

8.8
MODE Scanner Testbed (Top View)

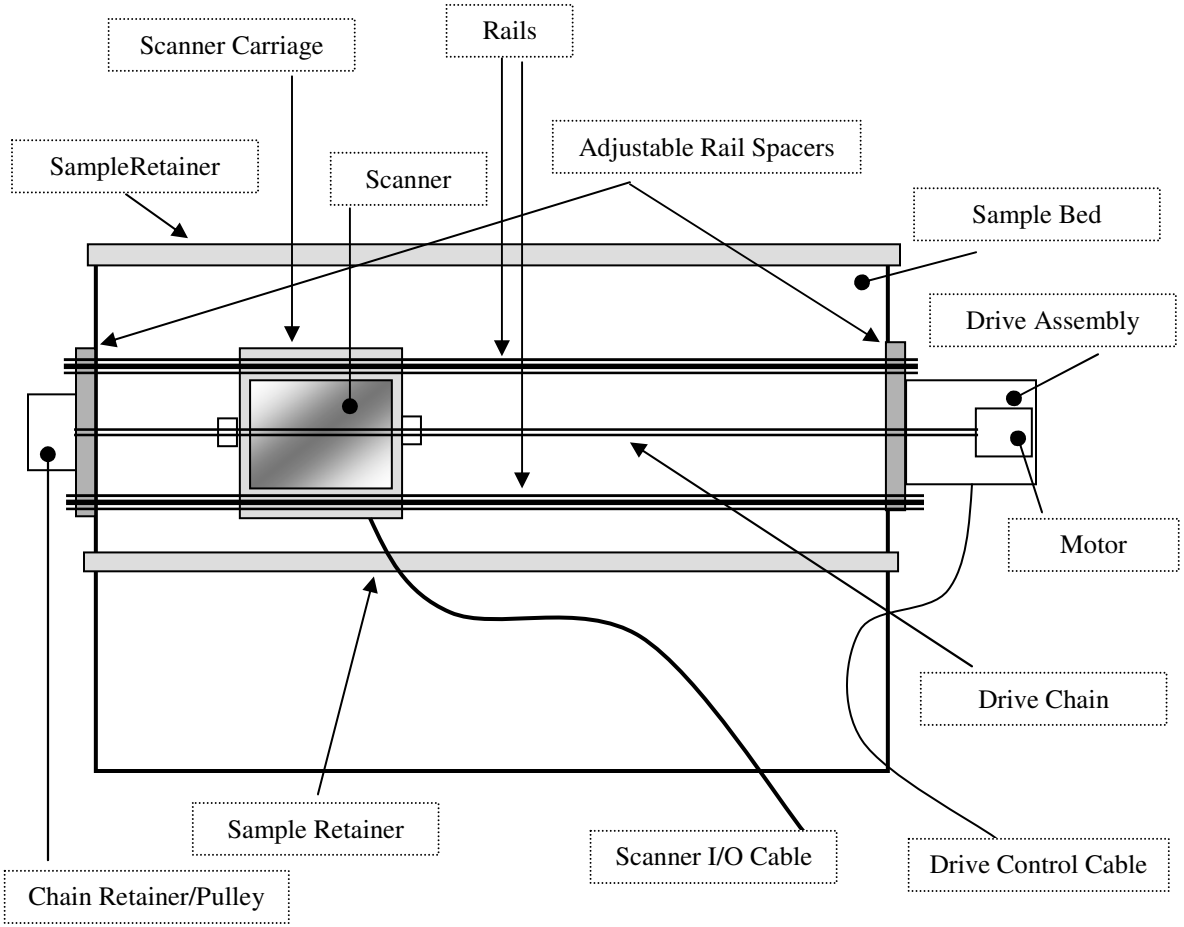

8.9
MODE Scanner Testbed (End View)

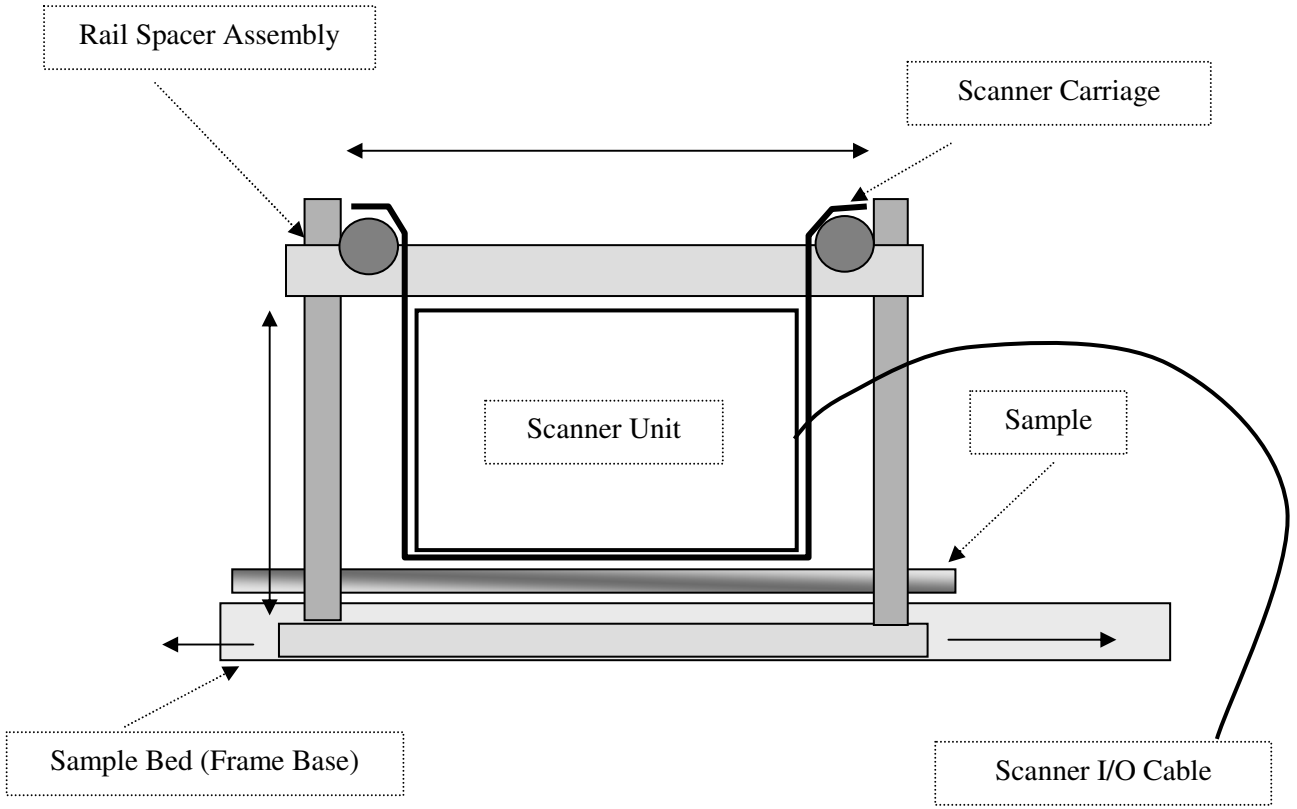

8(a)

9. Recapitulation and Conclusions

Following a particular line of reasoning has required opening several doors, often simultaneously, and peering into different rooms at the same time…

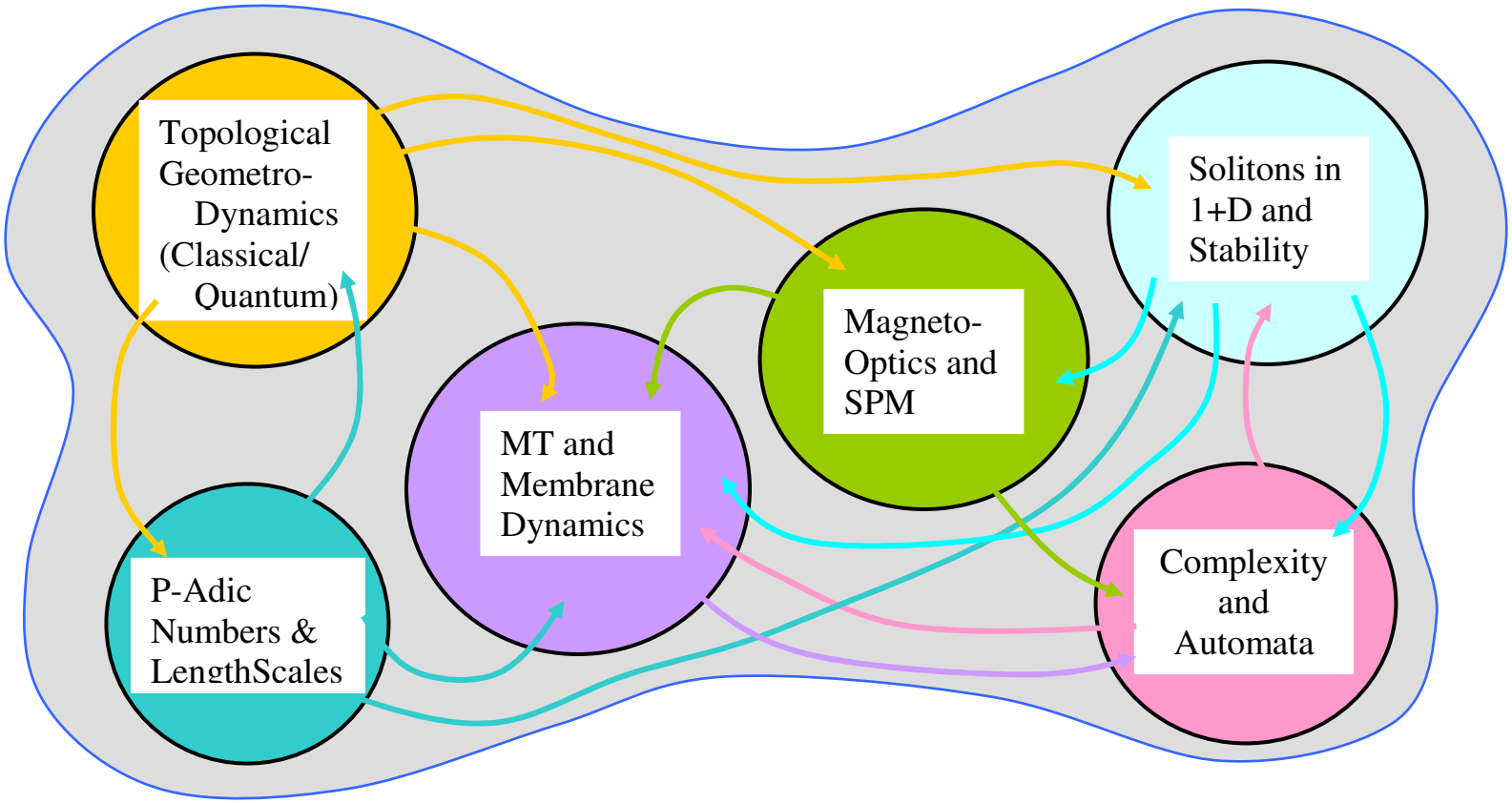

CREDITS

I. Bogolubsky (LCTA, JINR, Dubna)
L. Brizhik (ITP, Kiev)
J. Chen (Grad student, BME)
A. Chernovenkis (MODIS)
R. Freer (Commonwealth Biotechnologies)
M. Gilardi (Lab Assistant)
E. Henderson (Iowa State)
S. Japee (Grad student, BME)
M. Pitkanen (Univ. of Helsinki)
V. Sanyuk (People's Friendship Univ., Moscow)
P. Werbos (NSF)